

Fe_2O_3 Particles Coated with Silica Using TEOS

Satoshi Sato,* Ryoji Takahashi, Toshiaki Sodesawa, and Rieko Tanaka

Department of Materials Technology, Faculty of Engineering, Chiba University, Yayoi, Inage, Chiba 263-8522

(Received August 29, 2002)

Fine particles of SiO_2-coated Fe_2O_3 were prepared by depositing silica on an iron(III) hydroxide precipitate using tetraethoxysilane (TEOS). The silica deposition proceeded under mild conditions at 20 °C; crystallization hardly occurred and silica loading was controlled by the amount of TEOS charged, whereas the precipitate crystallized to a mixture of FeO(OH) and α-Fe_2O_3 under hydrothermal conditions. The specific surface area of the SiO_2-coated Fe_2O_3 increased with silica loading, and exceeded 280 $m^2\ g^{-1}$ even after calcination at 500 °C. The silicate species deposited on the precipitate of iron(III) hydroxide prevented the primary particles from agglomerating during calcination, resulting in the high surface area and hard reducibility of the SiO_2-Fe_2O_3.

It is known that silica-gel particles grow in aqueous alkaline solution, and that the dissolution-deposition of SiO_2 alters a rough surface of silica gel to a smooth one to decrease the surface energy.[1] Both the dissolution rate and the solubility of SiO_2 increase with increasing pH of the solution[2] and temperature.[3] The dissolution of silica from borosilicate glass, which is widely used for glass vessels, also proceeds in a basic solution. We have reported that silica dissolved from the glass vessel in a basic solution deposits on $ZrO(OH)_2$ particles in our recent work[4] on the preparation of high surface-area zirconia by aging $ZrO(OH)_2$ in a basic solution, which was originally reported by Chuah et al.[5,6] We found that the silica deposited on $ZrO(OH)_2$ prevented the agglomeration of particles during calcination.[4]

We proposed that the dissolution-deposition process of SiO_2 could be used to prepare silica-coated metal oxides. Then, using this process, we prepared high surface-area SiO_2–ZrO_2.[4] As a fresh precipitate of $ZrO(OH)_2$ was heated with several pieces of silica glass chips in a basic solution under hydrothermal (HT) conditions at 100 °C, the silica component dissolved from the glass deposits on the precipitate. The specific surface area (hereinafter abbreviated to SA) of the resulting SiO_2–ZrO_2 increased with the silica loading, and exceeded 240 $m^2\ g^{-1}$, even after calcination at 500 °C.

In preliminary tests, it was found that silica deposited on several metal hydroxides, such as nickel(II), iron(III), and tin(IV) hydroxides, under HT conditions. The SA of SiO_2-covered NiO and SnO_2 exceeded 200 $m^2\ g^{-1}$ in the same way as the SiO_2–ZrO_2.[4] It was also found that the silica deposited on $Ni(OH)_2$ prevented the agglomeration of NiO particles.[7] In contrast, the SA of SiO_2-covered Fe_2O_3 was as small as 67 $m^2\ g^{-1}$. Since the pure iron(III) hydroxide dried at 110 °C had a high SA of $>$ 200 $m^2\ g^{-1}$, we expected that SiO_2-covered Fe_2O_3 could have a high SA under different silica-deposition conditions.

The purpose of this work is, therefore, to prepare fine particles of Fe_2O_3 by different methods and to explore the character of the resultant SiO_2-Fe_2O_3. After we have clarified silica deposition on the hydroxide under HT conditions in ammonia solution with silica glass chips at 100 °C, we investigate the fine particles of SiO_2-coated Fe_2O_3 prepared under mild conditions using tetraethoxysilane (TEOS) at 20 °C. We also examine the reduction behavior of the resulting SiO_2-Fe_2O_3.

Experimental

Sample Preparation. All reagents were supplied by Wako Pure Chemical Industry Ltd., Japan. An iron(III) hydroxide precipitate was obtained by adding 10 wt% of an iron(III) nitrate solution (51 g) into 5.0 mol dm^{-3} of an ammonia solution (194 g). The fresh precipitate containing 12.6 mmol-Fe, which corresponded to 1 g of the resulting Fe_2O_3, was used for the following silica deposition.

A fresh hydroxide precipitate was placed in a poly(tetrafluoroethylene) vessel together with 25 cm^3 of the mother solution at a pH of 9.8–9.9, and was heated at 100 °C for 24–192 h in a pressure vessel with a volume of 50 cm^3. In the HT process for silica deposition, several pieces of silica glass tube (SiO_2 content, 100%; outside diameter, 6 mm; inside, 4 mm; length, 20–40 mm) with the total surface area adjusted to ca. 190 cm^2 were immersed in the solution. The precipitate collected by filtration was dried at 110 °C for 24 h to obtain a SiO_2-FeO(OH) sample. It was then calcined in air at 500 °C for 3 h at a heating rate of 1 K min^{-1} to obtain a SiO_2-Fe_2O_3 sample.

Another silica deposition was examined using a TEOS solution. A fresh hydroxide precipitate prepared by the above-mentioned method was dropped in a glass vessel with an ethanol solution (40 cm^3) containing TEOS (0.17–1.39 g, ex. 0.693 g corresponds to 200 mg of silica), after filtration and removal of ammonia by washing with water. The hydroxide precipitate suspended in the solution was stirred for a prescribed period, until a white precipitate caused by abrupt hydrolysis and polymerization of TEOS had not been observed when an aqueous NaOH solution was added into the extracted supernatant solution. Then, the precipitate was collected by filtration, dried, and calcined in the same manner as the HT post-treatment mentioned above.

Characterization. A specific surface area (SA) of the sample was determined by the BET method using the N_2 adsorption isotherm at -196 °C in a conventional volumetric gas adsorption apparatus. Prior to adsorption, the samples were heated in a vacuum

at 110 and 300 °C for 1 h for the dried and calcined samples, respectively. According to a method reported by Dollimore and Heal,[8] the pore-size distribution was calculated using the desorption branch of the N_2 adsorption–desorption isotherm measured at −196 °C by Omnisorp 100CX (Coulter, U.S.A.).

The X-ray diffraction (XRD) spectra of samples were recorded on an M18XHF (Mac Science, Japan) with Cu Kα radiation (λ = 0.154178 nm). An X-ray fluorescence (XRF) analysis was performed on an MESA-500 (Horiba, Japan).

A temperature-programmed reduction (TPR) measurement was performed from 30 to 900 °C at a heating rate of 5 K min^{-1}. A sample (ca. 20 mg) was fixed in a quartz tube with quartz wool. A mixture of H_2/N_2 (= 1/9) was flowed at atmospheric pressure at a flow rate of 10 cm^3 min^{-1}, and H_2 consumed during the program was monitored with a thermal-conductivity detector.[9,10]

A temperature-programmed desorption (TPD) measurement of adsorbed benzaldehyde was made in an N_2 flow of 50 cm^3 min^{-1} from 250 to 800 °C at a heating rate of 10 K min^{-1}. Prior to the adsorption of benzaldehyde, a sample (ca. 20 mg) fixed in a quartz tube with quartz wool was heated in the N_2 flow at 500 °C for 1 h. After the sample bed had been cooled to 250 °C, five pulses of benzaldehyde with each pulse of 10 mm^3 were injected in the N_2 flow. Benzaldehyde desorbed from the sample was monitored on a flame-ionization detector. It has been reported that benzaldehyde is adsorbed not on silica, but on iron(III) oxide.[11,12] Thus, we can calculate the surface density of the adsorbed benzaldehyde, which means the exposure of iron(III) oxide on the surface. A commercial silica, CARiACT Q-10 (SA = 295 m^2 g^{-1}) supplied by Fuji Silycia, was used as a reference of a silica surface.

Results

Silica Deposition under HT Conditions. The solubility of silica can be negligible in a 5.0 mol dm^{-3} NH_3 solution at 100 °C.[4] Thus, the amount of silica dissolved can be regarded as silica loading. Table 1A shows silica loading calculated from the weight loss of silica glass chips during the HT process in a NH_3 solution at 100 °C. The silica loading did not increase with passing the HT-process time after 24 h, and was saturated at a loading of ca. 50 mg per gram of the resulting Fe_2O_3.

Table 1A also shows the SA values of SiO_2–FeO(OH) and SiO_2–Fe_2O_3 samples. An original hydroxide precipitate dried at 110 °C had a high SA of 213 m^2 g^{-1}, although it reduced its SA to 24 m^2 g^{-1} after calcination at 500 °C. The SA value of SiO_2–FeO(OH) decreased in the HT process, whereas no significant change was observed during calcination. Since the SA values of SiO_2–Fe_2O_3 calcined at 500 °C were three-times as large as that of pure Fe_2O_3, the SiO_2 coating in the HT process had a small effect on the increase in the SA of Fe_2O_3. In contrast to the silica-coated samples, pure hydroxide decreased the SA during the HT process in the absence of silica glass for 48 h; the resulting Fe_2O_3 had a SA of 22 m^2 g^{-1}, which was close to that of a non-HT sample. It is speculated that the hydroxide particles agglomerate during the HT process.

Figure 1 depicts the XRD profiles of SiO_2-coated samples prepared under the HT conditions. The iron(III) hydroxide precipitate had a low crystallinity, which consisted of FeO(OH) (Fig. 1a). When an amorphous-like precipitate was treated under the HT conditions without silica glass, it transformed into crystalline FeO(OH) and α-Fe_2O_3 (Fig. 1c). The SiO_2–FeO(OH) precipitate also showed diffraction peaks of FeO(OH) and α-Fe_2O_3 (Fig. 1b). In samples of SiO_2–Fe_2O_3 calcined at 500 °C (Fig. 1d), major peaks were observed at 2θ = 33.2, 35.6, 40.9, 49.5, 54.0, 62.4, and 64.0 degrees, which were assigned as planes of (104), (110), (113), (024), (116),

Table 1. Physical Properties of SiO_2–Fe_2O_3 Prepared by Silica Deposition

Reaction period/h	SiO_2 loading /mg $g_{Fe_2O_3}^{-1}$	Specific surface area[a]/m^2 g^{-1}		Particle size of Fe_2O_3[b]/nm
		SiO_2–FeO(OH)	SiO_2–Fe_2O_3	
0	0	213 (0.20)	24 (0.14)	43
(A) HT process with silica glass at 100 °C[c]				
24	50	58	69	—
48	41	66	73	21
144	56	56	73	—
48[d]	0	—	22	—
(B) TEOS deposition process at 20 °C[e]				
48	100	320	169 (0.25)	10
96	200	346	230 (0.34)	10
144	300	386	262 (0.40)	10
336	400	405	285	10

a) Specific surface area calculated by BET method; numbers in parentheses indicate pore volume (cm^3 g^{-1}) calculated by nitrogen adsorption at −196 °C. b) Average particle size of Fe_2O_3 in the SiO_2–Fe_2O_3 calculated by Scherrer's equation using full width at half maximum of the peak at 2θ = 54.0°, assigned as (116) plane. c) Treated with hydrothermal process in the NH_3 (5 mol dm^{-3}) solution containing glass chips at 100 °C. The SiO_2 loading is measured by weight decrease of silica glass chips during the HT process. d) HT process in the absence of silica glass. e) Prepared by immersing the precipitate in TEOS ethanol solution at 20 °C. The SiO_2 loading is calculated from the charged TEOS as it completely deposited on the surface.

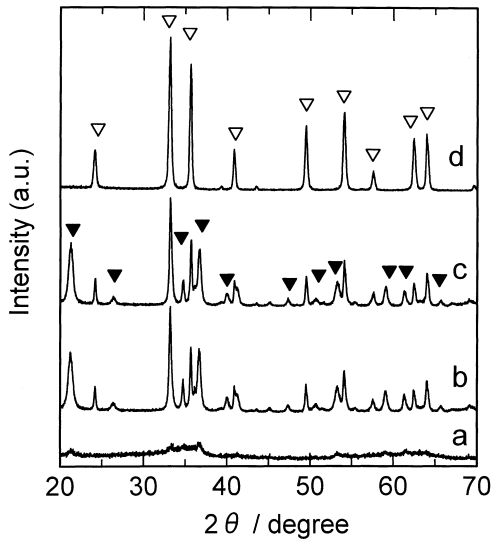

Fig. 1. XRD profiles of SiO_2–FeO(OH) samples prepared under HT conditions. a, Non-hydrothermal sample; b, HT treatment with glass for 48 h; c, HT treatment without glass for 48 h; d, sample b was calcined at 500 °C. ▽: α-Fe_2O_3, ▼: FeO(OH).

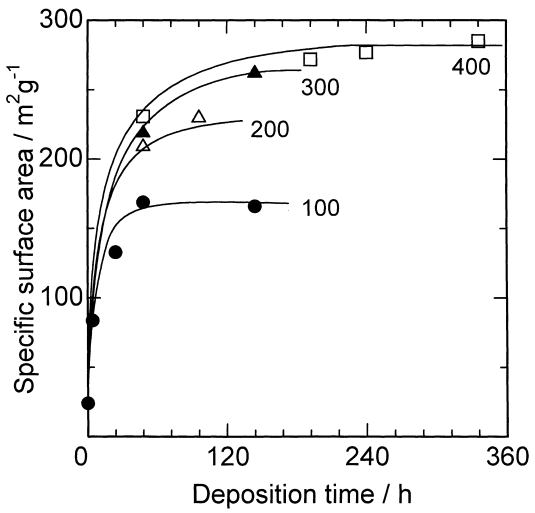

Fig. 2. Changes in specific surface area of SiO_2–Fe_2O_3 with TEOS deposition time. Iron(Ⅲ) hydroxide was immersed in TEOS solution at 20 °C. Numbers in the figure indicate the amount of silica (mg $g_{Fe_2O_3}^{-1}$) charged in the solution as TEOS.

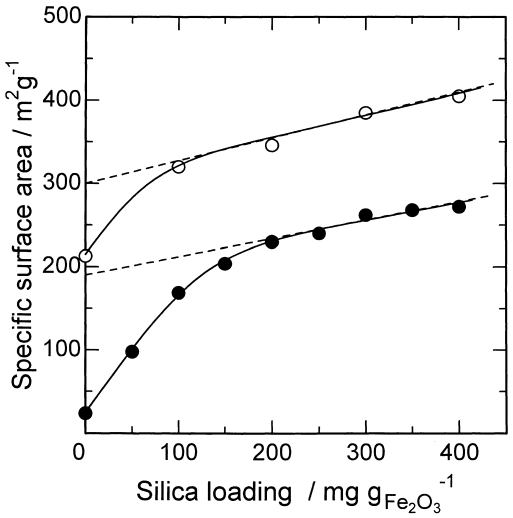

Fig. 3. Changes in specific surface area with silica loading for samples prepared using TEOS at 20 °C. ○, SiO_2–FeO(OH) dried at 110 °C; ●, SiO_2–Fe_2O_3 calcined at 500 °C.

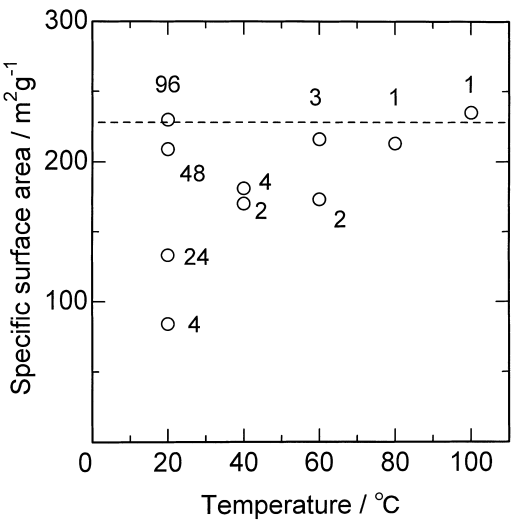

Fig. 4. Specific surface area of SiO_2–Fe_2O_3 prepared using TEOS at different temperatures. Numbers indicate the reaction time (h) of TEOS deposition. TEOS (0.693 g, which corresponds to 200 mg of silica) was used for the silica deposition on 1 g of Fe_2O_3.

(214), and (300) of α-Fe_2O_3, hematite, respectively. The XRD results indicate that an amorphous-like hydroxide precipitate was crystallized to FeO(OH) and α-Fe_2O_3 during the HT process, and that FeO(OH) was decomposed into α-Fe_2O_3 during calcination.

Silica Deposition Using TEOS. TEOS in the coating solution was surely consumed during deposition, and all of the TEOS disappeared from the solution for some periods. In a reference, no consumption of TEOS was observed in the absence of iron(Ⅲ) hydroxide. Figure 2 shows the changes in the SA of SiO_2–Fe_2O_3 with the deposition time in which an iron(Ⅲ) hydroxide was immersed in a TEOS/ethanol solution at 20 °C. The SA of the samples became saturated after an appropriate period, after which no TEOS was detected in the supernatant solution. Thus, the charged TEOS was completely deposited on the hydroxide. In both the TEOS deposition and the HT process with silica glass, we tested the XRF analysis for several SiO_2–Fe_2O_3 samples (spectra not shown). An X-ray signal from Si atom was observed, and its intensity was comparable to the calculated silica loading, while pure Fe_2O_3 showed no Si-XRF signal.

Figure 3 shows the changes in the SA of SiO_2–FeO(OH) and SiO_2–Fe_2O_3 with silica loading. The SA values are listed in Table 1B. A high SA value of hydroxide was maintained in the SiO_2–FeO(OH) samples, and the SA increased with in-

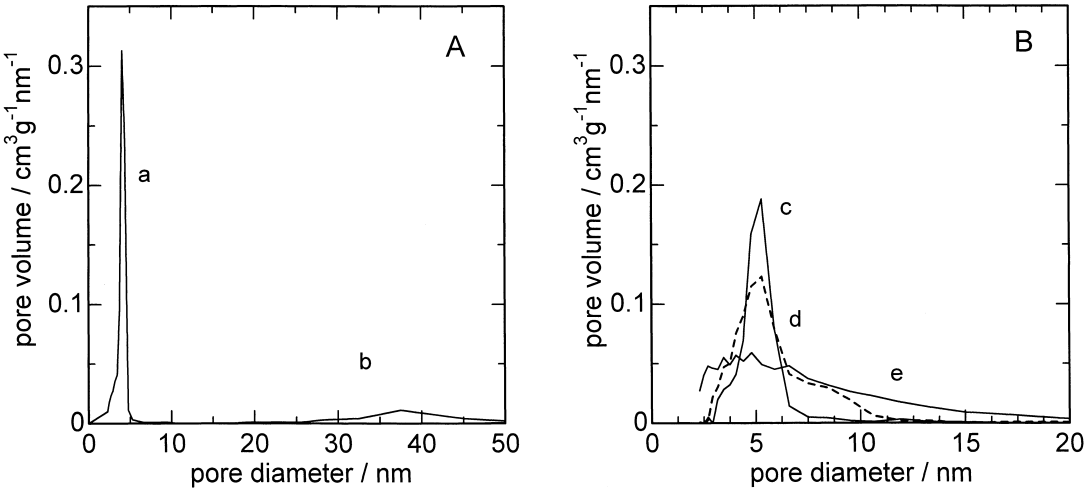

Fig. 5. Pore-size distribution of (A) pure Fe_2O_3 and (B) SiO_2–Fe_2O_3 prepared using TEOS at 20 °C. a, hydroxide precipitate dried at 110 °C; b, pure Fe_2O_3; c, silica loading of 100; d, 200; e, 300 mg $g_{Fe_2O_3}{}^{-1}$.

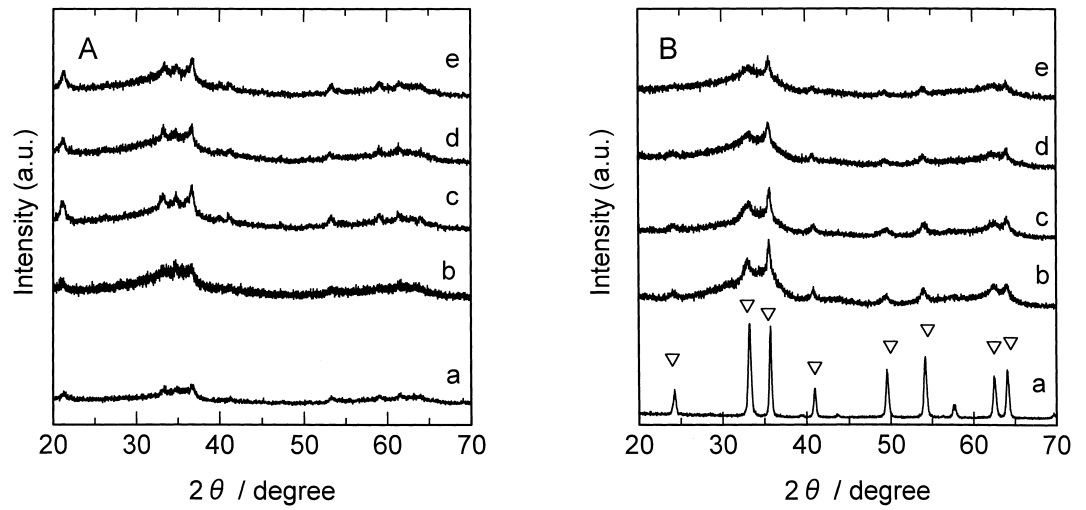

Fig. 6. XRD profiles of (A) SiO_2–FeO(OH) and (B) SiO_2–Fe_2O_3 samples prepared using TEOS at 20 °C. a, silica loading of 0; b, 100; c, 200; d, 300; e, 400 mg $g_{Fe_2O_3}{}^{-1}$. ▽: α-Fe_2O_3.

creasing the silica loading. The SA of the SiO_2–Fe_2O_3 samples also increased with increasing the silica loading. Figure 4 shows the effect of the temperature in the TEOS deposition process. It is obvious that a high SA of > 200 m^2 g^{-1} was rapidly attained at a higher deposition temperature; the high SA was obtained at 80 °C for 1 h.

Figure 5 depicts the pore-size distribution of SiO_2–Fe_2O_3 prepared in TEOS deposition at 20 °C. At low silica loading, the SiO_2–Fe_2O_3 sample had a pore-size distribution similar to that of pure iron(III) hydroxide. The distribution shifted to the large pore-size side with silica loading. Table 1 also lists the pore volume, which increased with increasing silica loading.

Figure 6 depicts the XRD profiles of samples prepared in the TEOS deposition. Both SiO_2–FeO(OH) and SiO_2–Fe_2O_3 were partially crystallized. The diffraction peaks of the crystallite grains were assigned as the α-Fe_2O_3 phase. Also, the XRD pattern observed in the sample prepared at 100 °C for 1 h (Fig. 4) was comparable to that of SiO_2–Fe_2O_3 prepared at 20 °C (profile not shown). Table 1 also lists the average particle size of the α-Fe_2O_3 phase in the samples, which was calculated by Scherrer's equation using the broadening of the (116) peak. It is obvious that the SiO_2–Fe_2O_3 samples prepared using TEOS consist of small primary particles of α-Fe_2O_3.

Figure 7 shows TPD profiles of the adsorbed benzaldehyde. The benzaldehyde adsorbed on the SiO_2–Fe_2O_3 samples was desorbed at around 450 °C, while the other adsorbed on a commercially available silica was at around 580 °C. The amount of adsorbed benzaldehyde was normalized by the specific surface area to calculate the density of the adsorbed benzaldehyde. Figure 8 shows the change in the density of the adsorption sites of benzaldehyde. Benzaldehyde adsorbed on pure Fe_2O_3 with a density of 0.75 nm^{-2}, while it adsorbed on the commercial silica at a small density of ca. 0.02 nm^{-2}. The adsorption density decreased to ca. 0.1 nm^{-2} with increasing the silica loading. This indicates that the fraction of the Fe_2O_3 surface decreases.

Figure 9 shows TPR profiles of SiO_2–Fe_2O_3 calcined at 500 °C. Pure Fe_2O_3 was readily reduced below 700 °C. The SiO_2–

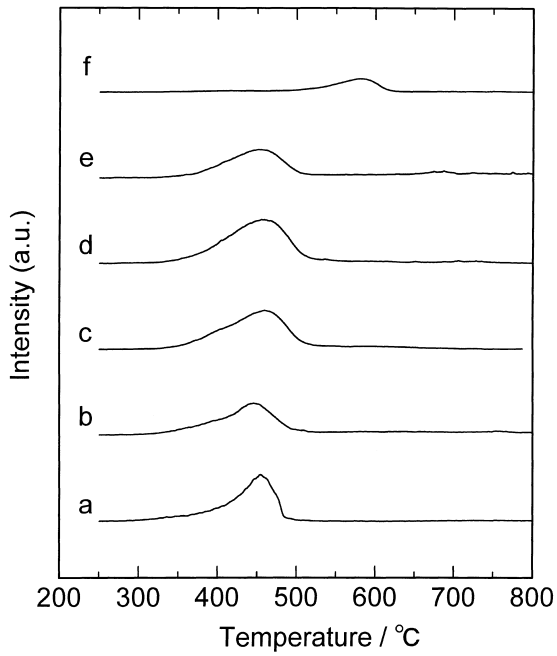

Fig. 7. TPD profiles of benzaldehyde adsorbed on SiO_2–Fe_2O_3 samples prepared using TEOS at 20 °C. a, pure Fe_2O_3; b, silica loading of 50; c, 150; d, 200; e, 300 mg $g_{Fe_2O_3}^{-1}$; f, commercial silica gel.

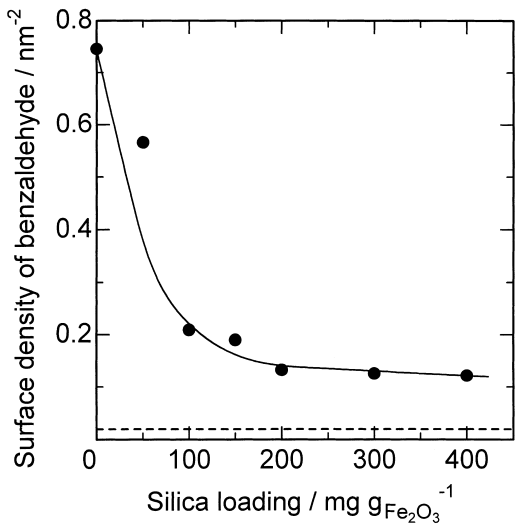

Fig. 8. Change in density of adsorption site of benzaldehyde. The density was calculated from the amount of adsorbed benzaldehyde (Fig. 7) per unit surface area (Fig. 3).

Fe_2O_3 required a very high temperature to be reduced by hydrogen. A new peak appeared above 800 °C, and the irreducible species increased with increasing silica loading. This means that the SiO_2–Fe_2O_3 samples with higher silica loading are less reducible.

Discussion

Deposition of Silica. In the preparation of metal oxides, such as ZrO_2, NiO, and Fe_2O_3, the metal hydroxides precipitated in basic conditions have a high SA above 200 $m^2\ g^{-1}$. However, they lost the high SA in calcined bodies of oxide because of the aggregation and growth of the crystal phase of metal oxides. In our previous study on SiO_2–ZrO_2 and SiO_2–NiO prepared in the HT process, the high SA of SiO_2-coated hydroxide was retained even after being calcined at 500 °C, and the core ZrO_2 and NiO were amorphous and of low crystallinity, respectively.[4,7] Although silica deposition is observed on the iron(III) hydroxide particles, the aggregation of particles and the crystallization to FeO(OH) and α-Fe_2O_3 are observed under HT conditions (Fig. 1).

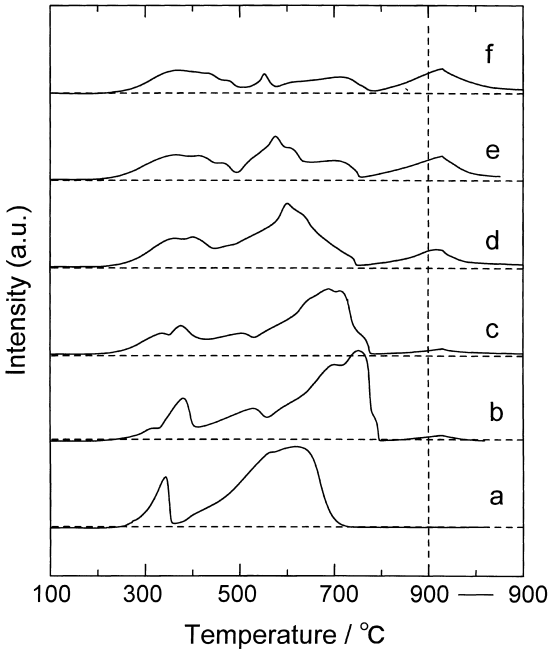

Fig. 9. TPR profiles of SiO_2–Fe_2O_3 samples prepared using TEOS at 20 °C. a, pure Fe_2O_3; b, silica loading of 50; c, 100; d, 200; e, 300; f, 400 mg $g_{Fe_2O_3}^{-1}$.

The temperature in aging clearly affects the aggregation of hydroxide and crystallization (Figs. 1 and 6). Since the deposition rate of silica onto hydroxide was not very fast under the HT conditions at 100 °C using silica glass, the hydroxide precipitate aggregated and crystallized into FeO(OH) and α-Fe_2O_3 before silica had deposited. This is the reason why SiO_2–Fe_2O_3 treated under the HT conditions at 100 °C lost the high SA of the original hydroxide. In the deposition process using TEOS, the deposition rate at 20 °C is as slow as the dissolution rate of silica under the HT conditions at 100 °C. However, the silica deposited from TEOS effectively works as an obstacle to prevent the aggregation of hydroxide during calcinations, because no hydroxide precipitate aggregates at a low temperature of 20 °C.

The deposition rate of silica from TEOS is greatly affected by the temperature (Fig. 4). At a higher deposition temperature of TEOS, a high SA is attained for short periods. This is simply related to the silica deposition rate. The core hydroxide does not aggregate even at 100 °C because of the fast silica deposition from TEOS; silica deposits on the surface before the core hydroxide crystallizes.

Incidentally, sol–gel techniques have been applied to the coating of iron(III) oxide using silicon alkoxide.[13–15] In pio-

neering reports, coating was described as having been done under strongly basic[13,14] and acidic conditions,[15] so that the silicon alkoxide was hydrolyzed and condensed to silica aggregates. In a TEM measurement,[14] it was clearly observed that the silica layer covered the Fe_2O_3 particles, while the silica layer was too thick to be as large as the core particle size. It has been reported that silica-coated Fe_2O_3 has a high specific surface area, 297 $m^2\ g^{-1}$, after drying at 150 °C,[15] whereas no details are mentioned about the thermal resistance and the relation between the silica loading and the specific surface area of the coated particles. In this work, we did not use any catalysts for the hydrolysis of TEOS, and the silica deposition proceeded via a surface reaction between TEOS and the surface OH groups of FeO(OH). This is a significant difference between the present and pioneering studies.

Agglomeration of Iron(Ⅲ) Hydroxide and Oxide Particles. A gradual agglomeration of $ZrO(OH)_2$ precipitate was observed in pure ZrO_2 treated under the HT conditions at 100 °C.[4] The SA of a $ZrO(OH)_2$ sample dried at 110 °C decreased from 220 to 90 $m^2\ g^{-1}$ with increasing the HT period from 0 to 192 h. It is noted that the agglomeration of iron(Ⅲ) hydroxide proceeds much faster than that of $ZrO(OH)_2$ under the same HT conditions (Table 1A and Fig. 1). Pure hydroxide precipitate readily aggregates during the HT process in the absence of silica glass at 100 °C.

In silica deposition using TEOS, we do not have to worry about the agglomeration of the hydroxide precipitate. It is obvious that silica is deposited on hydroxide precipitates at a low temperature, at which the agglomeration and crystallization of hydroxide do not occur. It is advantageous that the reactive TEOS is readily deposited under mild conditions. The SA values of the samples increase with increasing silica loading (Fig. 3). In comparing SiO_2–FeO(OH) with SiO_2–Fe_2O_3, the SA of the former is always higher than that of the latter. This is simply explained by the difference in the density; the densities of Fe_2O_3 and FeO(OH) are 5.25 and 4.26 g cm^{-3}, respectively.[16] In a simple geometric calculation, the diameter (d) of a spherical particle is calculated to be $d = 6000/SA/\rho$ nm, where ρ is the density. Using the SA value of Y-intercept of Fig. 3, the d of Fe_2O_3 spherical particles with SA of 190 $m^2\ g^{-1}$ is calculated to be $d = 6.0$ nm, and that of FeO(OH) particles with 300 $m^2\ g^{-1}$ is $d = 4.7$ nm. In addition, the d of non-coated Fe_2O_3 particles with a SA of 24 $m^2\ g^{-1}$ is calculated to be $d = 48$ nm. Judging from the d values, the deposited silica prevents Fe_2O_3 particles from aggregating during calcination; the primary particle of hydroxide transforms into an Fe_2O_3 particle without aggregation during calcination. Actually, the average size of the Fe_2O_3 particles listed in Table 1 is consistent with the above discussion. Therefore, the high SA of an as-dried precipitate of SiO_2–FeO(OH) is maintained after calcination. A similar observation was found in previous SiO_2–ZrO_2 and SiO_2–NiO systems under the HT process in an aqueous alkaline solution.[4,7]

The vapor-phase deposition of silica on oxide supports has been studied: silica-coated catalysts, such as SiO_2–ZrO_2 and SiO_2–TiO_2, were prepared by depositing silica in the vapor phase,[17,18] while the SA of ZrO_2 and TiO_2 supports was smaller than 70 $m^2\ g^{-1}$. We also investigated alumina-supported silica and its usage for acid catalysis.[19–21] Even for the alumina with an SA of 200 $m^2\ g^{-1}$, the SA of support limits that of the resulting composite material in the vapor-phase deposition process. The present liquid-phase deposition process using TEOS and as-prepared metal hydroxide, however, has a great advantage: the high SA of the original hydroxide is retained under mild deposition conditions so as not to aggregate the primary particles of the support hydroxide.

Regarding high-surface-area SiO_2–ZrO_2,[4] we have considered a mechanism for preventing aggregation from sintering; an oxide layer with a different structure acts as an obstacle of aggregation of the core oxide particles during heating. A similar behavior has been reported for silica-alumina prepared by contacting silica with alumina; the alumina particles exhibit a heat resistance to sintering.[22,23] That is, the silica phase acts as an obstacle for the sintering of alumina particles because of the different crystal structure. Moreover, alumina supported on silica also prevents the agglomeration of the core silica under the HT conditions.[24] In the same way, the deposited silicate species prevents the Fe_2O_3 precursors from sintering.

Surface Structure and Reduction Behavior of SiO_2–Fe_2O_3. The TPD results indicate that the silica species covers the Fe_2O_3 surface, and that the surface character of Fe_2O_3 becomes closer to that of silica with an increase in the silica loading (Fig. 8). The difference in the TPD peak positions between pure silica and the SiO_2–Fe_2O_3 suggest that the adsorption sites of SiO_2–Fe_2O_3 can be attributed to the exposed Fe_2O_3 surface (Fig. 7).

The silica-coated Fe_2O_3 particles prepared by Ohmori and Matijevic were reduced by hydrogen at 450 °C, even at a high SiO_2/Fe_2O_3 weight ratio of 3.76, although it had a thick silica layer with a thickness of ca. 60 nm.[14] In their TEM observation, the Fe core shrinks in the thick silica shell, which seems to be stable while retaining a rigid structure during reduction.

The structure of the present SiO_2–Fe_2O_3 seems to be a core Fe_2O_3 covered with silica shell. Although the silica shell was not reduced by hydrogen, it did not protect the core Fe_2O_3 during reduction; a part of Fe_2O_3 in the samples was reduced. The silica shell would be partially composed of iron silicate. The silicate is an irreducible Fe_2O_3 species, which is reduced at temperatures higher than 800 °C according to the TPR profiles (Fig. 9). The TPR results show that the amount of irreducible Fe_2O_3 species increases with increasing silica loading. It is obvious that the irreducible Fe_2O_3 species readily forms during silica deposition, followed by the calcination.

Conclusions

We tried to prepare fine particles of SiO_2-coated Fe_2O_3 with a high SA by depositing silica on the iron(Ⅲ) hydroxide precipitate. When a fresh precipitate of the hydroxide was heated in a pressure vessel under hydrothermal (HT) conditions in an aqueous ammonia solution containing several pieces of silica glass chips at 100 °C, the precipitate crystallized to a mixture of FeO(OH) and α-Fe_2O_3 together with growth of the particle size. Although the silica components dissolved from silica glass were deposited on the precipitate, the silica loading was not controlled by the HT period. The SA values of the resulting SiO_2–Fe_2O_3 were smaller than those of pure hydroxide dried at 110 °C. Thus, the HT process was not efficient for preparing fine particles of SiO_2-coated Fe_2O_3.

We then replaced silica glass chips with tetraethoxysilane (TEOS) as a silica source. Another precipitate of the hydroxide was contacted with a TEOS/ethanol solution at 20 °C. Silica components were deposited on the precipitate through TEOS decomposition, and the silica loading was controlled by the amount of TEOS. The SA of the SiO_2–Fe_2O_3 prepared by TEOS deposition increased with silica loading, and exceeded 280 $m^2\ g^{-1}$ even after calcination at 500 °C. In contrast to pure Fe_2O_3, which readily aggregated during heating, the silicate species deposited on the surface of the original precipitate particles prevented the primary particles from agglomerating during calcination, resulting in the high surface-area SiO_2–Fe_2O_3. In the pore-size distribution, the pore volume increased with the silica loading. The deposition rate of silica from TEOS varied with the temperature. The increase in the temperature shortened the period to complete the silica deposition; the SA of a sample prepared at 20 °C for 96 h equaled that prepared at 80–100 °C for 1 h.

References

1 R. K. Iler, "The Chemistry of Silica," Wiley, New York, (1979), p. 30.

2 P. W. J. Wijnen, T. P. M. Beelen, J. W. de Haan, C. P. J. Rummens, L. J. M. van de Ven, and R. A. van Santen, *J. Non-Cryst. Solids*, **109**, 85 (1989).

3 J. J. Mazer and J. V. Walter, *J. Non-Cryst. Solids*, **170**, 32 (1994).

4 S. Sato, R. Takahashi, T. Sodesawa, S. Tanaka, K. Oguma, and K. Ogura, *J. Catal.*, **196**, 190 (2000).

5 G. K. Chuah, S. Jaenicke, S. A. Chong, and K. S. Cham, *Appl. Catal. A*, **145**, 267 (1996).

6 G. K. Chuah, S. Jaenicke, and B. K. Pong, *J. Catal.*, **175**, 80 (1998).

7 S. Sato, R. Takahashi, T. Sodesawa, N. Ichikuni, and H. Amano, *Bull. Chem. Soc. Jpn.*, **75**, 2297 (2002).

8 D. Dollimore and G. R. Heal, *J. Appl. Chem.*, **14**, 109 (1964).

9 T. Nakayama, N. Ichikuni, S. Sato, and F. Nozaki, *Appl. Catal. A*, **158**, 185 (1997).

10 S. Sato, R. Takahashi, T. Sodesawa, K. Yuma, and Y. Obata, *J. Catal.*, **196**, 195 (2000).

11 M. Niwa, Y. Matsuoka, and Y. Murakami, *J. Phys. Chem.*, **91**, 4519 (1987).

12 M. Niwa, K. Suzuki, M. Kishida, and Y. Murakami, *Appl. Catal.*, **67**, 297 (1991).

13 M. Ohmori and E. Matijevic, *J. Colloid Interface Sci.*, **150**, 594 (1992).

14 M. Ohmori and E. Matijevic, *J. Colloid Interface Sci.*, **160**, 288 (1993).

15 M. Klotz, A. Ayral, C. Guizard, C. Menager, and V. Cabuil, *J. Colloid Interface Sci.*, **220**, 357 (1999).

16 "Handbook of Chemistry and Physics," 82nd ed, ed by D. R. Lide. CRC Press, Boca Raton, Florida (2001).

17 T. Jin, T. Okuhara, and J. M. White, *J. Chem. Soc., Chem. Commun.*, **1987**, 1248.

18 M. Niwa, N. Katada, and Y. Murakami, *J. Catal.*, **134**, 340 (1992).

19 S. Sato, M. Toita, Y. Q. Yu, T. Sodesawa, and F. Nozaki, *Chem. Lett.*, **1987**, 1535.

20 S. Sato, M. Toita, T. Sodesawa, and F. Nozaki, *Appl. Catal.*, **62**, 73 (1990).

21 S. Sato, T. Sodesawa, F. Nozaki, and H. Shoji, *J. Mol. Catal.*, **66**, 343 (1991).

22 B. E. Yoldas, *J. Mater. Sci.*, **11**, 465 (1976).

23 N. Katada, H. Ishiguro, K. Muto, and M. Niwa, *Chem. Vap. Deposition*, **1**, 54 (1995).

24 S. Sato, R. Takahashi, T. Sodesawa, A. Miura, C. Kobayashi, and K. Ogura, *Phys. Chem. Chem. Phys.*, **3**, 885 (2001).